Low-PAPR Joint Transmit/Received SC-FDE Transmission using Time-Domain Selected Mapping

Amnart Boonkajay* and Fumiyuki Adachi†
Department of Communications Engineering, Graduate School of Engineering, Tohoku University
6-6-05 Aza-Aoba, Aramaki, Aoba-ku, Sendai, Miyagi, 980-8579 Japan
Email: *amnart@mobile.ecei.tohoku.ac.jp, †adachi@ecei.tohoku.ac.jp

***Abstract*— Transmit filtering, transmit equalization, precoding, or power allocation increases the peak-to-average power ratio (PAPR) of transmit single-carrier (SC) signal due to change in frequency-domain spectrum. Recently, we proposed a frequency-domain based selected mapping (FD-SLM) for suppressing the increased PAPR introduced by the transmit frequency-domain equalization (Tx-FDE). However, FD-SLM provides minor contribution when computational complexity is considered. In this paper, we are motivated by the fact that a "bad" arrangement of modulated symbols in a transmission block leads to high peak power, and propose a time-domain phase rotation called time-domain SLM (TD-SLM). PAPR and BER performances when using the proposed TD-SLM are evaluated by computer simulation and are compared to conventional joint Tx/Rx SC-FDE and joint Tx/Rx SC-FDE with FD-SLM.**

Keywords*— Single-carrier (SC) transmission, peak-to-average power ratio (PAPR), selected mapping (SLM), frequency-domain equalization (FDE)

I. INTRODUCTION

Broadband wireless channel is characterized as a frequency-selective fading channel, in which inter-symbol interference (ISI) degrades the bit-error rate (BER) performance [1]. Multi-carrier transmission e.g. orthogonal frequency division multiplexing (OFDM) is robust against fading, but its high peak-to-average power ratio (PAPR) is the main drawback [2]. On the other hand, single-carrier (SC) transmission [3] is more attractive for uplink transmissions, e.g., in LTE-Advanced (LTE-A) system, because of lower PAPR, while the use of frequency-domain equalization (FDE) can take advantage of channel frequency selectivity to improve the BER performance [4].

SC signal can be generated by inserting discrete Fourier transform (DFT) into conventional OFDM transmitter [5], which provides flexibility of signal manipulations in frequency domain, e.g., mapping and filtering. SC using joint transmit/receive FDE (joint Tx/Rx SC-FDE) [6] is a low-complexity SC transmission technique, where transmit FDE (Tx-FDE) and receive FDE (Rx-FDE) are jointly optimized. Even though joint Tx/Rx SC-FDE provides better BER performance compared to conventional SC-FDE, it increases the PAPR because of changes in spectrum shape, implying that PAPR reduction algorithm is necessary. We recently proposed a frequency-domain based selected mapping (FD-SLM) technique for SC-FDE and joint Tx/Rx SC-FDE [7], which can be considered as a promising PAPR reduction technique for SC signal since it provides small signal overhead and no signal distortion. Signal candidates for selection are generated by applying phase rotation to frequency-domain signal prior to inverse fast Fourier transform (IFFT). FD-SLM provides up to 2 dB PAPR reduction for joint Tx/Rx SC-FDE. However, a contribution of PAPR reduction is minor when computational complexity is considered [8].

The peak power of SC-FDE waveform depends on the data symbol sequence in a block [9]. A "bad" sequence leads to high peak power [10, 11]. This fact motivates us to generate candidates for SLM by applying phase rotation in time domain instead of in frequency domain. In this paper, we propose a time-domain based SLM (TD-SLM) for joint Tx/Rx SC-FDE. PAPR and BER performances when using the proposed TD-SLM are evaluated by computer simulation and are compared to conventional joint Tx/Rx SC-FDE and joint Tx/Rx SC-FDE with FD-SLM. It is also shown in the paper that the Tx-FDE and Rx-FDE weights in [6] can be used with TD-SLM without modification and no BER performance degradation is produced as far as phase rotation is perfectly known at the receiver ($\log_2 U$-bit side information needs to be informed to the receiver side, where U is number of candidates).

The remaining of this paper is organized as follows. Section II proposes TD-SLM. The transceiver model for joint Tx/Rx SC-FDE using TD-SLM is described in Section III. Section IV provides performance evaluation, and Section V concludes the paper.

II. TD-SLM ALGORITHM

SLM [7, 8] has been introduced as a frequency-domain based PAPR reduction technique with relatively small overhead and without distortion on waveform. In this paper, we introduce a new SLM technique which the phase rotation is applied in time-domain, called TD-SLM. TD-SLM algorithm is simply depicted by Fig. 1.

Assuming that time-domain transmit vector $\mathbf{s}$ is represented by $\mathbf{s}=[s(0),s(1),\ldots,s(N_c-1)]^{\mathrm{T}}$, PAPR of the time-domain transmit signal calculated over an oversampled transmission block is expressed by

$$PAPR(\mathbf{s}) = \frac{\max\{|s(n)|^2, n = 0, \frac{1}{V}, \frac{2}{V}, ..., N_c - 1\}}{E[|s(n)|^2]}, \quad (1)$$

where V is oversampling factor.

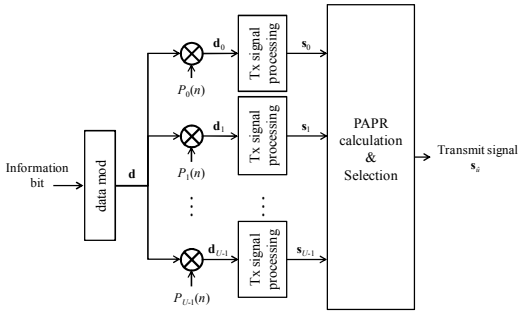

Fig. 1. TD-SLM algorithm.

A set of U different $N_c \times N_c$ diagonal phase-rotation sequence matrices $\mathbf{P}_u = diag[P_u(0),\ldots,P_u(N_c-1)]$, $u=0\sim U-1$ is defined, and time-domain transmit block candidates are generated by multiplying the phase-rotation matrices to the time-domain transmit block $\mathbf{d}=[d(0),d(1),\ldots,d(N_c-1)]^T$, obtaining $\mathbf{d}_u=\mathbf{P}_u\mathbf{d}$. Note that $\mathbf{P}_0$ is set to be all "1" sequence for the first candidate as a representative of original transmit block, where the other candidates are generated either in a deterministic or random approach. We assume the phase-rotation sequence to be real number in order to reduce the number of complex-valued multiplication, and unit-magnitude in order to meet the transmit power constraint, that is $P_u(n)=\pm 1$, $n=0\sim N_c-1$. In this paper, we use a set of phase-rotation sequences generated from 4095-bit pseudonoise (PN) sequence, which is confirmed in [7, 12] that it provides the same performance in SLM as random sequence, while the sequence itself is deterministic.

The instantaneous PAPR of time-domain transmit signal candidates after passing through transmit signal processing $\mathbf{s}_u=[s_u(0),\ldots,s_u(N_c-1)]^T$ are calculated based on (1), and the selected transmit signal $\mathbf{s}_{\hat{u}}=[s_{\hat{u}}(0),\ldots,s_{\hat{u}}(N_c-1)]^T$ with the corresponding selected phase-rotation sequence index $\hat{u}$, whose provides the lowest PAPR among U candidates, is selected by the following criterion.

$$\hat{u} = \arg \min_{u=0,1,\ldots,U-1} PAPR(\mathbf{s}_u = \mathbf{F}_{N_c}^H \mathbf{W}_T \mathbf{F}_{N_c} \mathbf{P}_u \mathbf{d}) . \quad (2)$$

Note that matrix and vector representations for transmit signal processing in joint Tx/Rx SC-FDE in (2) will be described in more details in Section III.

III. TD-SLM FOR JOINT TX/RX SC-FDE

Single-user N_c-length block transmission with N_g-length of cyclic prefix insertion is assumed. DFT and its inverse operation are used in the transceiver for reaching frequency-domain processing, where Tx-FDE weight is applied as one-tap multiplication. In a system using the proposed TD-SLM, time-domain symbols are mapped by multiplying with phase-rotation sequence prior to applying DFT. Transceiver of joint Tx/Rx SC-FDE equipped with TD-SLM is shown by Fig. 2.

A. Transmitter

Transmitter of joint Tx/Rx SC-FDE equipped with TD-SLM is shown in Fig. 2(a). We begin with a block of N_c data-modulated symbols $\mathbf{d}=[d(0),d(1),\ldots,d(N_c-1)]^T$. The block $\mathbf{d}$ is used to generate U candidates for SLM $\mathbf{d}_u$ by multiplying different phase-rotation sequence. The u-th transmit block candidate block is expressed by

$$\mathbf{d}_u = \mathbf{P}_u \mathbf{d} , \quad (3)$$

where $\mathbf{P}_u \equiv diag[P_u(0),P_u(1),\ldots,P_u(N_c-1)]$ represents phase rotation matrix. The detail of phase-rotation sequence $P_u(n)$ is already discussed in Sect. II. Then, each transmission block candidate is transformed into frequency domain by N_c-point DFT, yielding frequency components of the u-th candidate $\mathbf{D}_u=[D_u(0),D_u(1),\ldots,D_u(N_c-1)]^T$ as

$$\mathbf{D}_u = \mathbf{F}_{N_c} \mathbf{P}_u \mathbf{d} , \quad (4)$$

where N_c-point DFT matrix $\mathbf{F}_{N_c}$ is expressed by

$$\mathbf{F}_{N_c} = \frac{1}{\sqrt{N_c}} \begin{bmatrix} 1 & 1 & \cdots & 1 \\ 1 & e^{\frac{-j2\pi(1)(1)}{N_c}} & \cdots & e^{\frac{-j2\pi(1)(N_c-1)}{N_c}} \\ \vdots & \vdots & \ddots & \vdots \\ 1 & e^{\frac{-j2\pi(N_c-1)(1)}{N_c}} & \cdots & e^{\frac{-j2\pi(N_c-1)(N_c-1)}{N_c}} \end{bmatrix} . \quad (5)$$

Next, $\mathbf{D}_u$ is multiplied by Tx-FDE weight matrix, which is a $N_c \times N_c$ diagonal matrix $\mathbf{W}_T = diag[W_T(0),\ldots,W_T(N_c-1)]$, obtaining the frequency component after applying Tx-FDE of the u-th candidate $\mathbf{S}_u=\mathbf{W}_T\mathbf{D}_u$. Note that Tx-FDE weight calculation is described in Sect. III-*C*.

After that, $\mathbf{S}_u$ is transformed back into time domain by N_c-point inverse fast Fourier transform (IFFT) matrix $\mathbf{F}_{N_c}^H$. PAPR calculation is applied in order to search and select the time-domain transmit signal with the lowest PAPR based on (2) as $\mathbf{s}_{\hat{u}}=[s_{\hat{u}}(0),s_{\hat{u}}(1),\ldots,s_{\hat{u}}(N_c-1)]^T$. The selected time-domain transmit signal based on TD-SLM $\mathbf{s}_{\hat{u}}$ is expressed by

$$\mathbf{s}_{\hat{u}} = \mathbf{F}_{N_c}^H \mathbf{W}_T \mathbf{F}_{N_c} \mathbf{d}_{\hat{u}} = \mathbf{F}_{N_c}^H \mathbf{W}_T \mathbf{F}_{N_c} \mathbf{P}_u \mathbf{d} . \quad (6)$$

Finally, the last N_g samples of transmit block are copied as a cyclic prefix (CP) and inserted into the guard interval (GI), then a CP-inserted signal block of N_g+N_c samples is transmitted.

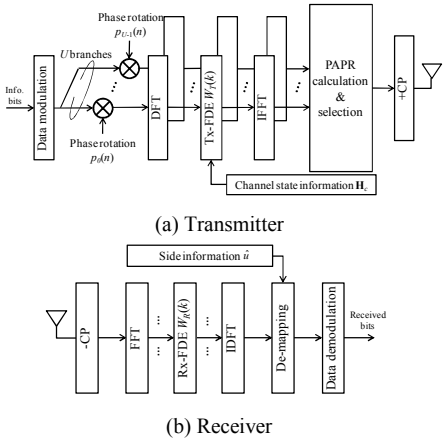

Fig. 2. Transmission system models of joint Tx/Rx SC-FDE with TD-SLM

B. Receiver

The propagation channel is assumed to be a symbol-spaced L-path frequency-selective block fading channel [1], where its impulse response is given by

$$h(\tau)=\sum_{l=0}^{L-1}h_l\delta(\tau-\tau_l)\,, \tag{7}$$

where h_l and τ_l are complex-valued path gain and time delay of the l-th path, respectively. $\delta(\cdot)$ is the delta function. Time-domain received signal after CP removal, $\mathbf{r}_{\hat{u}}=[r_{\hat{u}}(0),r_{\hat{u}}(1),...,r_{\hat{u}}(N_c-1)]^T$, is expressed by

$$\mathbf{r}_{\hat{u}}=\sqrt{\frac{2E_s}{T_s}}\mathbf{h}\mathbf{s}_{\hat{u}}+\mathbf{n}\,. \tag{8}$$

where $\mathbf{s}_{\hat{u}}=\mathbf{F}_{N_c}^H\mathbf{W}_T\mathbf{F}_{N_c}\mathbf{P}_{\hat{u}}\mathbf{d}$ is obtained from (6), E_s is symbol energy, and $\mathbf{n}$ is noise vector in which each element is zero-mean additive white Gaussian noise (AWGN) having the variance $2N_0/T_s$ with T_s is symbol duration and N_0 being the one-sided noise power spectrum density. Channel response matrix $\mathbf{h}$ is a circular matrix representing time-domain channel response which is

$$\mathbf{h}=\begin{bmatrix} h_0 & & & h_{L-1} & \cdots & h_1 \\ h_1 & \ddots & & & \ddots & \vdots \\ \vdots & & h_0 & \mathbf{0} & & h_{L-1} \\ h_{L-1} & & h_1 & \ddots & & \\ & \ddots & \vdots & & \ddots & \\ \mathbf{0} & & h_{L-1} & \cdots & \cdots & h_0 \end{bmatrix}. \tag{9}$$

The received signal vector $\mathbf{r}_{\hat{u}}$ is transformed into frequency domain by N_c-point FFT, obtaining the frequency-domain received signal $\mathbf{R}_{\hat{u}}$ as

$$\begin{aligned}\mathbf{R}_{\hat{u}} &= \sqrt{\frac{2E_s}{T_s}}\mathbf{F}_{N_c}\mathbf{h}\mathbf{F}_{N_c}^H\mathbf{W}_T\mathbf{D}_{\hat{u}}+\mathbf{F}_{N_c}\mathbf{n} \\ &= \sqrt{\frac{2E_s}{T_s}}\mathbf{H}_c\mathbf{W}_T\mathbf{D}_{\hat{u}}+\mathbf{N}\end{aligned}\,. \tag{10}$$

where the frequency-domain channel response $\mathbf{H}_c$ is

$$\mathbf{F}_{N_c}\mathbf{h}\mathbf{F}_{N_c}^H=diag[H_c(0),...,H_c(N_c-1)]\equiv\mathbf{H}_c\,. \tag{11}$$

Rx-FDE $\mathbf{W}_R=diag[W_R(0),\ldots,W_R(N_c-1)]$ is applied at the receiver as a joint cooperation with Tx-FDE in order to reduce the effect from frequency-selective fading. The equalized signal $\hat{\mathbf{D}}_{\hat{u}}=\mathbf{W}_R\mathbf{R}_{\hat{u}}$ where $\hat{\mathbf{D}}_{\hat{u}}=[\hat{D}_{\hat{u}}(0),\hat{D}_{\hat{u}}(1),\ldots,\hat{D}_{\hat{u}}(N_c-1)]^T$ is later transformed back into time domain by N_c-point inverse DFT (IDFT), yielding time-domain signal before de-mapping $\hat{\mathbf{d}}_{\hat{u}}=[\hat{d}_{\hat{u}}(0),\hat{d}_{\hat{u}}(1),\ldots,\hat{d}_{\hat{u}}(N_c-1)]^T$ as

$$\hat{\mathbf{d}}_{\hat{u}}=\mathbf{F}_{N_c}^H\hat{\mathbf{D}}_{\hat{u}}=\mathbf{F}_{N_c}^H\mathbf{W}_R\mathbf{R}_{\hat{u}}+\mathbf{F}_{N_c}^H\mathbf{W}_R\mathbf{N}\,. \tag{12}$$

Note that the derivation of $\mathbf{W}_R$ will be described in Sect. III-*C*.

Finally, de-mapping is applied to time-domain signal after applying Rx-FDE in order to obtain the original time-domain transmission block. De-mapping is simply done by multiplying $\hat{\mathbf{d}}_{\hat{u}}$ with the Hermitian transpose of selected phase-rotation sequence, obtaining time-domain received vector $\hat{\mathbf{d}}=[\hat{d}(0),\hat{d}(1),\ldots,\hat{d}(N_c-1)]^T$ as

$$\hat{\mathbf{d}}=\mathbf{P}_{\hat{u}}^H\hat{\mathbf{d}}_{\hat{u}}\,. \tag{13}$$

From (13), it is observed that the receiver needs to know which phase-rotation sequence is selected as a sequence providing the lowest PAPR; otherwise an accurate de-mapping cannot be achieved and consequently degrades the BER performance. This indicates that up to $\log_2 U$ bits of explicit side information is indispensable (as shown in Fig. 2(b)).

C. FDE Weights Calculation

Performance of joint Tx/Rx SC-FDE in aspect of BER performance has been extensively discussed in [6]. In this subsection, we expect to use the proposed FDE weights in [6] without modifications even though TD-SLM is employed.

Joint FDE weights calculation begins from the receiver. By using the minimum mean-square error (MMSE) criterion [4, 6] where the mean-square error (MSE) is calculated between frequency-domain transmitted and received signal. An error vector $\mathbf{e}$ is given by

$$\begin{aligned}\mathbf{e} &= \hat{\mathbf{D}}_{\hat{u}}-\sqrt{\frac{2E_s}{T_s}}\mathbf{D}_{\hat{u}} \\ &= \sqrt{\frac{2E_s}{T_s}}(\mathbf{W}_R\mathbf{H}_c\mathbf{W}_T-\mathbf{I}_{N_c})\mathbf{D}_{\hat{u}}+\mathbf{W}_R\mathbf{N}\end{aligned}\,. \tag{14}$$

The MSE $e=tr[\mathbf{e}\mathbf{e}^H]$ is expressed as

$$\begin{aligned}tr[\mathbf{e}\mathbf{e}^H]=&\\ &tr[(\mathbf{W}_R\mathbf{H}_c\mathbf{W}_T-\mathbf{I}_{N_c})(\mathbf{W}_R\mathbf{H}_c\mathbf{W}_T-\mathbf{I}_{N_c})^H]E[\mathbf{D}_{\hat{u}}\mathbf{D}_{\hat{u}}^H]\\ &+\frac{E_s}{N_0}tr[\mathbf{W}_R\mathbf{W}_R^H]\end{aligned}\,. \tag{15}$$

However, $E[\mathbf{D}_u\mathbf{D}_u^H]=1$ for all u=0~U–1 since we assume $P_u(n)$=±1 for all n=0~N_c–1, which makes $\mathbf{d}_u$ retain data-modulated symbol property with $d(n)$ being independent and identically distributed (i.i.d.). Therefore, $E[\mathbf{D}_u\mathbf{D}_{\hat{u}}^H]$ can be neglected from (15), yielding the MSE function in (15) is exactly the same as in [6]. Rx-FDE $W_R(k)$ is determined by solving $\partial(tr[\mathbf{e}\mathbf{e}^H])/\partial(W_R(k))$ for a given $\mathbf{W}_T$. That is

$$W_R(k)=\frac{H_c^*(k)W_T^*(k)}{\left|H_c(k)W_T(k)\right|^2+\left(E_s/N_0\right)^{-1}}\,. \tag{16}$$

Substituting $W_R(k)$ back into (15) yields the MSE function becomes a function of $\mathbf{W}_T$, which is also identical to the MSE

function in [6]. This indicates that $\mathbf{W}_T$ in [6] can be used in transmission with TD-SLM without modification. $W_T(k)$ is expressed by

$$W_T(k) = \max\left[\left\{\sqrt{\frac{(E_s/N_0)^{-1/2}}{\sqrt{\kappa}|H_c(k)|}} - \frac{(E_s/N_0)^{-1}}{|H_c(k)|^2}\right\}, 0\right]. \quad (17)$$

Note that κ is a parameter selected to satisfy the transmit power constraint $(1/N_c)\sum_{k=0}^{N_c-1}|W_T(k)|^2 = 1$. It is also observed that the transmitter requires channel information.

TABLE I. SIMULATION PARAMETERS

Transmitter	Data modulation	SC-16QAM
	FFT/IFFT block size	$N_c = 64$
	Cyclic prefix length	$N_g = 16$
	Average transmit E_b/N_0	10 dB
	Transmit filtering	Square-root Nyquist (α=0), Tx-FDE
SLM parameters	Phase-rotation sequence type	4095-bit long PN
	SLM type	FD-SLM, TD-SLM
	# of candidates	U = 1(no SLM)~64
	Oversampling factor	$V = 8$
Channel	Fading	Frequency-selective block Rayleigh
	Power delay profile	Symbol-spaced 1-path, 4-path, 16-path (uniform)
Receiver	Channel estimation	Ideal
	Side information	Ideal
	FDE	Joint Tx/Rx FDE

IV. PERFORMANCE EVALUATION

Numerical and simulation parameters are summarized in Table 1. We assume 16-QAM block transmission with the number of available subcarriers N_c=64. System performance is evaluated in terms of PAPR, BER, and computational complexity.

A. PAPR Performance

PAPR performance is evaluated by examining the complementary cumulative distribution function (CCDF). Fig. 3 shows the comparison of PAPR performance of joint Tx/Rx SC-FDE using FD-SLM and TD-SLM for symbol-spaced L-path block Rayleigh fading channel (L=1,4, and 16). PAPR performance of joint Tx/Rx SC-FDE without SLM is also shown for comparison. It can be seen that both FD-SLM and TD-SLM can reduce the PAPR when U increases, where TD-SLM provides lower PAPR than FD-SLM in every number of candidates U. This is consistent with our motivation as generating candidates for SLM in time domain is better than in frequency domain, because bad symbol sequence can be altered to another sequence.

It is also observed that the PAPR performance gap between TD-SLM and FD-SLM decreases as L increases. The reason for this can be explained by referring to [13] as follows. The channel frequency-selectivity gets severer as L increases (when L=1, the channel becomes frequency-nonselective). Since Tx-FDE is proportional to the channel transfer function (see Eq. (17)), Tx-FDE becomes closer to a rectangular filter [14] when L=4 and becomes a rectangular filter when L=1. Hence, if the channel frequency-selectivity is not too strong, the symbol sequence has a predominant impact on PAPR than changing in frequency spectrum due to Tx-FDE [10-11]. TD-SLM achieves better PAPR reduction than FD-SLM in such a moderate channel frequency-selectivity case. This consideration supports our simulation results shown in Fig. 3.

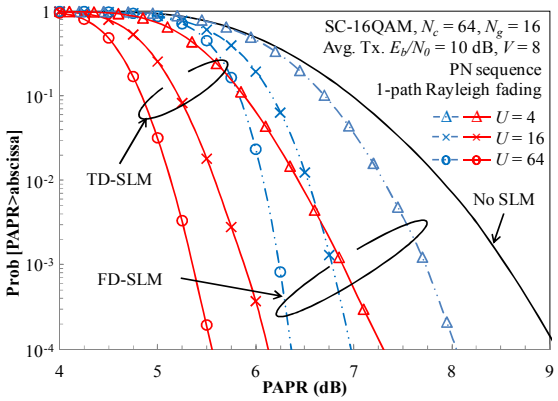

(a) 1-path Rayleigh fading

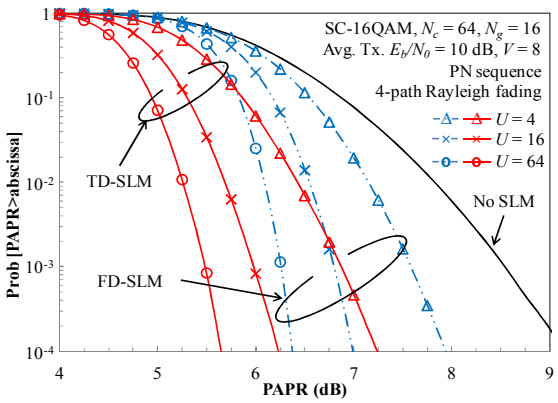

(b) 4-path Rayleigh fading

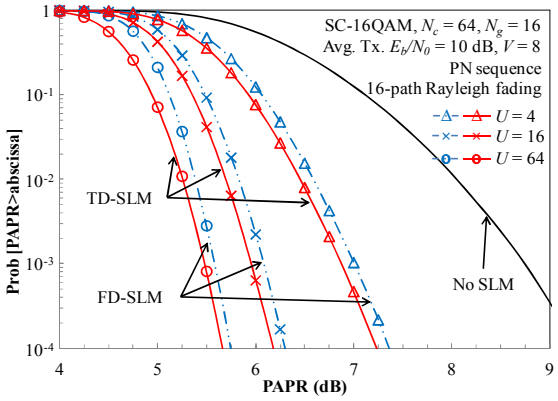

(c) 16-path Rayleigh fading

Fig. 3. PAPR performance of joint Tx/Rx SC-FDE.

B. BER Performance

Fig. 4 shows the BER performance as a function of average received bit energy-to-noise power spectrum density ratio E_b/N_0=0.25$(E_s/N_0)(1+N_g/N_c)$ for a symbol-spaced L-path

block Rayleigh fading channel (L=1,4, and 16). U=1 (no SLM) and 64 are considered. It confirms that the BER performances of joint Tx/Rx SC-FDE when TD-SLM is employed are the same as transmission without SLM as far as perfect side information is achieved. Joint Tx/Rx SC-FDE provides better BER performance than the conventional SC-FDE as a contribution from residual ISI reduction. In addition, it is seen that when L=1 and 4, the BER performance is worse than when L=16 due to lower path diversity gain [15].

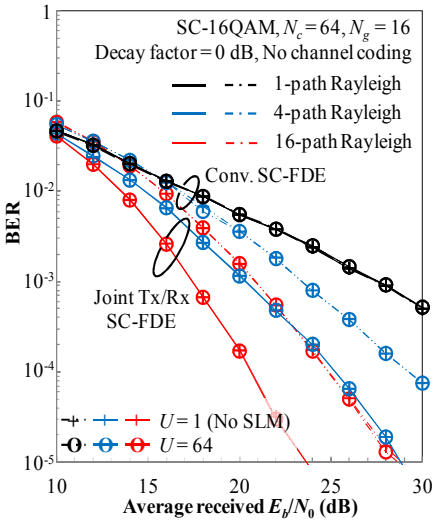

Fig. 4. BER performance of joint Tx/Rx SC-FDE.

TABLE II. COMPUTATIONAL COMPLEXITY

	No-SLM	FD-SLM[7]	TD-SLM
Phase rotation			
DFT (or FFT)	$N_c\log_2(N_c)$	$N_c\log_2(N_c)$	$U\times N_c\log_2(N_c)$
Tx-FDE weight calculation	$2N_c$	$2N_c$	$2N_c$
IFFT	$N_c\log_2(N_c)$	$U\times (VN_c)\log_2(VN_c)$	$U\times (VN_c)\log_2(VN_c)$
PAPR calculation		$U\times(VN_c)$	$U\times(VN_c)$

C. Computational Complexity

In this paper, computational complexity is evaluated by computing the number of complex-valued multiplications [16]. As indicated in [7], SLM requires high computational complexity due to an increasing of IFFT operation.

Table 2 shows the computational complexity of transmitters of joint Tx-Rx SC-FDE, joint Tx-Rx SC-FDE with FD-SLM, and joint Tx-Rx SC-FDE with TD-SLM. It is observed that TD-SLM requires more computational complexity since it requires U times of DFT operation. However, DFT can be replaced by FFT if the number of symbols per block is expressed in term of 2^n. Additional complexity from FFT operation is relatively small compared to IFFT operation for SLM since oversampling is not considered. For example, assuming N_c=64, U=64, and V=8, the additional complexity of TD-SLM compared to FD-SLM is less than 10%. This summarizes that the proposed TD-SLM provides better PAPR performance without performance degradation on BER, and with a small additional complexity compared to FD-SLM in [7].

V. CONCLUSION

In this paper, we proposed the TD-SLM for broadband joint Tx/Rx SC-FDE. The proposed TD-SLM generates transmit block candidates in time domain prior to DFT. It is confirmed in the paper that conventional Tx-FDE and Rx-FDE weights can be employed without modifications when TD-SLM is applied. Simulation results confirmed that the better PAPR performance is achieved without BER degradation compared to FD-SLM.

REFERENCES

[1] A. Goldsmith, *Wireless Communications*, Cambridge University Press, 2005.

[2] S. H. Han and J. H. Lee, "An Overview of Peak-to-Average Power ratio Reduction Techniques for Multicarrier Transmission," *Wireless Communications*, *IEEE*, vol.12, no.2, pp.56-65, April 2005.

[3] H. Sari, G. Karam, and I. Jeanclaude, "Transmission Techniques for Digital Terrestrial TV Broadcasting," *IEEE Commun. Mag.*, vol. 33, pp. 100-109, February 1995.

[4] D. Falconer, S. Ariyavisitakul, A. Benyamin-Seeyar, and B. Eidson, "Frequency Domain Equalization for Single-Carrier Broadband Wireless Systems," *Communications Magazine*, *IEEE*, vol.40, no.4, pp. 58-66, April 2002.

[5] H. Wu, and T. Haustein, "Radio Resource Management for the Multi-User Uplink Using DFT-Precoded OFDM," *in Proc. IEEE International Conference on Communications (ICC 2008)*, May 2008.

[6] K. Takeda, and F. Adachi, "Joint Iterative Transmit/Receive FDE&FDIC for Single-Carrier Block Transmissions," *IEICE Trans. Commun.*, vol. E94-B, no. 5, pp. 1396-1404, May 2011.

[7] A. Boonkajay, T. Obara, T. Yamamoto, and F. Adachi, "Selective Mapping for Broadband Single-Carrier Transmission Using Joint Tx/Rx MMSE-FDE," *in Proc. IEEE 24th International Symposium on Personal Indoor and Mobile Radio Communications (PIMRC 2013)*, Sept. 2013.

[8] H. Gacanin, and F. Adachi, "Selective Mapping with Symbol Re-mapping for OFDM/TDM Using MMSE-FDE," *in Proc. IEEE 68th Vehicular Technology Conference (VTC-Fall)*, Sept. 2008.

[9] S. L. Miller and R. J. O'Dea, "Peak Power and Bandwidth Efficient Linear Modulation," *IEEE Trans. Commun.*, vol. 46, no. 12, pp. 1639-1648, December 1998.

[10] Dov Wulich and Lev Goldfield, "Bound of the Distribution of Instantaneous Power in Single Carrier Modulation," *IEEE Trans. Wireless Commun.*, vol. 4, no. 4, pp. 1773-1778, July 2005.

[11] Vincent K. N. Lau, "Average of Peak-to-Average Ratio (PAR) of IS95 and CDMA2000 Systems – Single Carrier," *IEEE Commun. Lett.*, vol. 5, no. 4, pp. 160-162, April 2001.

[12] N. Ohkubo, and T. Ohtsuki, "Design Criteria for Phase Sequences in Selected mapping," *IEICE Trans. Commun.*, vol. E86-B, no. 9, pp. 2628-2636, Sept. 2003.

[13] A. Boonkajay, and F. Adachi, "Time-Domain Selective Mapping Technique for Filtered SC-FDE," *IEICE Technical Report,* vol. 114, no. 164, RCS2014-91, pp. 13-18, July 2014.

[14] Y. Akaiwa, *Introduction to Digital Mobile Communication*, 1st ed., Wiley, 1997.

[15] F. Adachi, T. Sao, and T. Itagaki, "Performance of multicode DS-CDMA using frequency domain equalization in a frequency selective fading channel," *IEE Electronics Lett.*, vol. 39, No.2, pp. 239-241, Jan. 2003.

[16] K. Tenma, T. Yamamoto, K. Lee, and F. Adachi, "2-step QRM-MLBD for Broadband Single-carrier Transmission," *IEICE Trans. Commun.*, vol. E95-B, no. 4, pp. 1366-1374, April 2012.